

Large CP violation in charmed baryon decays

Xiao-Gang He^{1,2,*} and Chia-Wei Liu^{1,2,†}

¹*Tsung-Dao Lee Institute, Shanghai Jiao Tong University, Shanghai 200240, China*

²*Key Laboratory for Particle Astrophysics and Cosmology (MOE)
 Shanghai Key Laboratory for Particle Physics and Cosmology,
 Shanghai Jiao Tong University, Shanghai 200240, China*

(Dated: May 9, 2024)

We present our study of CP violation in two-body weak decays of antitriplet charmed baryons. In the standard model, the $\Delta c = 1$ quark level interactions inducing CP violation for the relevant decays can be grouped into two types, one proportional to the CKM matrix elements $\lambda_d = V_{ud}V_{cd}^*$ and another $\lambda_b = V_{us}V_{cs}^*$. Recent studies have shown that with $SU(3)_F$ flavor symmetry, the decay amplitudes, including their strong phases, can be determined by data if contributions from λ_b are neglected. However, the λ_b terms must be retained to create interferences that induce CP violation. Some of them can be recovered in the framework of $SU(3)_F$ flavor symmetry, and the CP-violating rate asymmetry A_{CP} is predicted to be of the order of $\mathcal{O}(10^{-4})$. We find that final state re-scattering effects, which link hadronic matrix elements proportional to λ_d and λ_b , can help recover the missing terms. The re-scattering effects can enhance CP violation by an order of magnitude, with $A_{CP}(\Xi_c^0 \rightarrow pK^-) - A_{CP}(\Xi_c^0 \rightarrow \Sigma^+\pi^-)$ being as large as 1.87×10^{-3} . This makes it promising to observe CP violation for the first time in baryon decays.

The study of CP violation is fundamentally important. It is closely related to the baryon asymmetry in our universe (BAU) [1]. BAU suggests the need to go beyond the standard model (SM), as the CP violation from the Cabibbo-Kobayashi-Maskawa (CKM) mixing matrix [2] is too small to explain data. Where the new CP-violating source comes from is still unknown. The SM should be tested in all possible ways. Systems containing a charm quark may host some interesting surprises for CP violation tests, such as the CP-violating rate asymmetries of $D^0 \rightarrow \pi^+\pi^-$, K^+K^- observed at LHCb [3, 4], which are an order of magnitude larger than short-distance (SD) expectations [5]. Although there are speculations taking this as a signal for new physics beyond the SM [6, 7], it has also been argued that if long-distance (LD) contributions are properly taken into account, the SM can accommodate this large CP-violating effect [8–10]. A similar enhancement may also occur in other charmed particle decays. To this end, we propose to test CP violation in the charm sector using antitriplet charmed baryon (\mathbf{B}_c) decays into a low-lying octet baryon (\mathbf{B}) and a pseudoscalar meson (P), $\mathbf{B}_c \rightarrow \mathbf{B}P$. This may lead to the first discovery of CP violation in baryon decays.

The amplitudes of $\mathbf{B}_c \rightarrow \mathbf{B}P$ can be parameterized as $\mathcal{M} = -i\bar{u}(F - G\gamma_5)u_c$, where F and G are related to the S wave and P wave, respectively, and $u_{(c)}$ is the Dirac spinor of $\mathbf{B}_{(c)}$. If CP were conserved, F would flip sign and G would remain invariant under the CP transformation. One can construct the CP-violating rate asymmetry A_{CP} and polarization asymmetry A_{CP}^α as

$$A_{CP} = \frac{\mathcal{B} - \bar{\mathcal{B}}}{\mathcal{B} + \bar{\mathcal{B}}}, \quad A_{CP}^\alpha = \frac{\alpha + \bar{\alpha}}{2}. \quad (1)$$

Here, $\mathcal{B}(\bar{\mathcal{B}})$ and $\alpha(\bar{\alpha})$ represent the branching fraction and the polarization parameter for the particle (antiparticle), respectively. In terms of parameters in \mathcal{M} , α is equal to $2\kappa \text{Re}(F^*G)/(|F|^2 + \kappa^2|G|^2)$ with $\kappa = p_f/(E_f + M_f)$, where $M_{f(i)}$ and M_P are the respective masses of $\mathbf{B}_{(c)}$ and P , and $p_f(E_f)$ is the 3-momentum (energy) of \mathbf{B} in the rest frame of \mathbf{B}_c . Besides α there are two additional Lee-Yang parameters β and γ in $\mathbf{B}_c \rightarrow \mathbf{B}P$ [11]. Similar CP-violating observables can be constructed accordingly for them. Their measurements require polarized \mathbf{B}_c and the experimental measurements are more involved. We will concentrate on A_{CP} and A_{CP}^α here.

The effective Lagrangian \mathcal{L}_{eff} (or Hamiltonian $\mathcal{H}_{eff} = -\mathcal{L}_{eff}$) responsible for the $\Delta c = 1$ transition at the quark level is given by [12]

$$\mathcal{L}_{eff} = -\frac{G_F}{\sqrt{2}} \left[\sum_{q,q'=d,s} V_{cq}^* V_{uq'} (C_1 Q_1^{qq'} + C_2 Q_2^{qq'}) - \lambda_b \sum_{i=3\sim 6} C_i Q_i \right] + (H.c.), \quad (2)$$

where $Q_1^{qq'} = (\bar{u}\gamma^\mu(1 - \gamma_5)q')(\bar{q}\gamma_\mu(1 - \gamma_5)c)$, $Q_2^{qq'} = (\bar{q}\gamma^\mu(1 - \gamma_5)q')(\bar{u}\gamma_\mu(1 - \gamma_5)c)$, $Q_{3\sim 6}$ are the penguin operators, G_F is the Fermi constant, $C_{1,2}$ ($C_{3,4,5,6}$) are the Wilson coefficients for the tree (SD penguin) operators and $\lambda_q = V_{cq}^* V_{uq}$.

In order to have non-vanishing values for direct CP-violating observable A_{CP} , it requires at least two different weak CP-violating phases accompanied by different strong phases. Without $K^0 - \bar{K}^0$ mixing it is not possible for Cabibbo favored (CF) or doubly Cabibbo suppressed (DCS) processes which are proportional to a single weak phase $V_{ud}V_{cs}^*$ or $V_{us}V_{cd}^*$, but possible for the singly Cabibbo suppressed (SCS) tree contributions proportional to λ_d or $\lambda_s = -\lambda_d - \lambda_b$. It is interesting to note that in $\Lambda_c^+ \rightarrow \Xi^0 K^+$ the BESIII collaboration found a

* hexg@sjtu.edu.cn

† chiaweiliu@sjtu.edu.cn

sizable strong phase [13] which is another needed ingredient for non-vanishing A_{CP} and A_{CP}^α .

The theoretical calculations, starting from the quark-level effective interaction, for the decays of charmed hadrons are challenging due to the strong interactions at the charm scale. No reliable results from first principle calculations have been obtained. Methods based on symmetry considerations, such as flavor $SU(3)_F$, can simplify these calculations in a model-independent manner and provide avenues to obtain results that can be compared with experimental data. For our purpose of analyzing $\mathbf{B}_c \rightarrow \mathbf{B} P$, this approach is an excellent starting point, as it has been demonstrated that $SU(3)_F$ predictions fit data well, and many related amplitudes can be determined from known data [14–21].

Under the $SU(3)_F$ the tree operators $Q_{1,2}$ transform as $\mathbf{15}$, $\overline{\mathbf{6}}$ and $\mathbf{3}$. The explicit tensor representations of the effective Lagrangian responsible for the CF and DCS can be found in Ref. [17]. For SCS, including terms proportional to λ_b , we obtain

$$\mathcal{L}_{eff}^{\text{SCS}} = -\frac{G_F}{\sqrt{2}} \sum_{\lambda=\pm} C_\lambda (\mathcal{H}_\lambda)_{ij}^{ij} \bar{q}_i \gamma^\mu (1 - \gamma_5) q^k \bar{q}_j \gamma_\mu (1 - \gamma_5) c, \quad (3)$$

where $C_\pm = (C_1 \pm C_2)/2$. The $SU(3)_F$ tensor $(\mathcal{H}_+)_{ij}^{ij}$ is defined by

$$\frac{\lambda_s - \lambda_d}{2} \mathcal{H}(\mathbf{15}^{s-d})_{ij}^{ij} + \lambda_b \left(\mathcal{H}(\mathbf{15}^b)_{ij}^{ij} + \mathcal{H}(\mathbf{3}_+)^i \delta_k^j + \mathcal{H}(\mathbf{3}_+)^j \delta_k^i \right), \quad (4)$$

while $(\mathcal{H}_-)_k^{ij}$ by

$$\frac{\lambda_s - \lambda_d}{2} \mathcal{H}(\overline{\mathbf{6}})_{kl} \epsilon^{lij} + 2\lambda_b \left(\mathcal{H}(\mathbf{3}_-)^i \delta_k^j - \mathcal{H}(\mathbf{3}_-)^j \delta_k^i \right). \quad (5)$$

By construction \mathcal{H}_+ and \mathcal{H}_- are symmetric and antisymmetric in the two upper indices. The tensor components of \mathcal{H}_\pm are derived by matching Eqs. (2) and (3). The non-zero ones are given as $\mathcal{H}(\overline{\mathbf{6}})_{23} = \mathcal{H}(\mathbf{15}^{s-d})_{12}^{12} = -\mathcal{H}(\mathbf{15}^{s-d})_{33}^{13} = -1$, $-2\mathcal{H}(\mathbf{15}^b)_{11}^{11} = 4\mathcal{H}(\mathbf{15}^b)_{22}^{12} = 4\mathcal{H}(\mathbf{15}^b)_{33}^{13} = 4\mathcal{H}(\mathbf{3}_-) = 4\mathcal{H}(\mathbf{3}_+) = -1$ and the others are obtained by $\mathcal{H}(\overline{\mathbf{6}})_{ij} = \mathcal{H}(\overline{\mathbf{6}})_{ji}$ and $\mathcal{H}(\mathbf{15})_k^{ij} = \mathcal{H}(\mathbf{15})_k^{ji}$. The emergency of $\mathcal{H}(\mathbf{3}_\pm)$ is important. Note the $\mathbf{15}$ representation contains components proportional to λ_b also after using $\lambda_d + \lambda_s + \lambda_b = 0$. The SD penguin operators $Q_{3\sim 6}$ transform under $SU(3)_F$ as $\mathbf{3}$ with $C_{3\sim 6}$ smaller than $C_{1,2}$ by an order of $\mathcal{O}(10^{-1})$ [22]. We will focus on effects from the $\mathbf{3}$ in $Q_{1,2}$ first and comment on those from $Q_{3\sim 6}$ at the end.

The effective interaction operators have been grouped according to their $SU(3)_F$ representations, we should also do so for the initial and final hadron states. The antitriplet $(\mathbf{B}_c)_i$ contains $(\Xi_c^0, \Xi_c^+, \Lambda_c^+)_i$, while the octet low-lying baryon and meson representations are labelled as \mathbf{B}_j^i and P_j^i including $\{p, n, \Lambda, \Sigma^{\pm,0}, \Xi^{0,-}\}$ and $\{\pi^{\pm,0}, \eta_8, K^{\pm,0}, \overline{K}^0\}$ as elements, respectively. Their explicit tensors can be found in Ref. [20]. For later convenient, we define $\mathbf{B}_c^{[ij]} \equiv (\mathbf{B}_c)_k \epsilon^{kij}$. Note that η_8 is a mixture of the physical η and η' , which will not be discussed here.

The effective Lagrangian at the hadron level is obtained by writing down all possible $SU(3)_F$ contractions among $(\mathbf{B}_c)_i$, $(\mathbf{B})_j^i$, $(P^\dagger)_j^i$ and tensors of $\mathcal{L}_{eff}^{\text{SCS}}$ with quark fields stripped off. For each contraction, we assign an unknown parameter. The effective Lagrangian at the hadron level is then given by [20]

$$\begin{aligned} \mathcal{L}_{\mathbf{B}_c \mathbf{B} P} &= (P^\dagger)_n^l \overline{\mathbf{B}}_m^k \left(\frac{\lambda_s - \lambda_d}{2} (F^{s-d})_{ijkl}^{mn} \mathbf{B}_c^{[ij]} + \lambda_b (F^b)_{kl}^{imn} (\mathbf{B}_c)_i \right) + (H.c.), \\ (F^{s-d})_{ijkl}^{mn} &= \tilde{f}^b \mathcal{H}(\overline{\mathbf{6}})_{il} \delta_k^n \delta_j^m + \tilde{f}^c \mathcal{H}(\overline{\mathbf{6}})_{ik} \delta_j^n (\delta^\dagger)_l^m + \tilde{f}^d \mathcal{H}(\overline{\mathbf{6}})_{kl} \delta_j^n (\delta^\dagger)_i^m + \tilde{f}^e \mathcal{H}(\mathbf{15}^{s-d})_{il}^{mn} \epsilon_{ijk}/2, \\ (F^b)_{kl}^{imn} &= \tilde{f}^e \mathcal{H}(\mathbf{15}^b)_{il}^{mn} \delta_k^i + \tilde{f}_3^b \delta_l^i \mathcal{H}(\mathbf{3})^m \delta_k^n + \tilde{f}_3^c \mathcal{H}(\mathbf{3})^i \delta_l^m \delta_k^n + \tilde{f}_3^d \mathcal{H}(\mathbf{3})^n \delta_l^m \delta_k^i, \end{aligned} \quad (6)$$

where we have recombined $\mathcal{H}(\mathbf{3}_+)$ and $\mathcal{H}(\mathbf{3}_-)$ into $\mathcal{H}(\mathbf{3}) = (1, 0, 0)$, and \tilde{f} are the $SU(3)_F$ amplitudes. Since the S and P waves share the same flavor structure, Eq. (6) holds after the substitution of $(F, \tilde{f}) \rightarrow (-G, \tilde{g})$ with \tilde{g} free parameters in P waves [20]. The Körner-Pattin-Woo (KPW) theorem [23] had been applied to eliminate several redundant terms associated with $\mathcal{H}(\mathbf{15})$.

In Table I, we list the values of $\tilde{f}^{b,c,d,e}$ and $\tilde{g}^{b,c,d,e}$ extracted from the experimental values of \mathcal{B} and α [20]. At the current stage of the $SU(3)_F$ fit, the strong phases are subject to a Z_2 ambiguity as \mathcal{B} and α are invariant under the sign flip of strong phases [20]. Future precise experiments on β will break this degeneracy. Since $\lambda_d \gg \lambda_b$, it is challenging to precisely extract λ_b contributions using CP-conserving quantities. We consider final state re-scattering (FSR) for the LD effects to determine λ_b

contributions later.

It is interesting to note that even if \tilde{f}_3 and \tilde{g}_3 are dropped, one can still have non-zero A_{CP} and A_{CP}^α from the first term in F^b by using amplitudes for $\mathbf{15}$ already determined from data in F^{d-s} . In this case A_{CP} and A_{CP}^α are proportional to $\lambda_b \tilde{f}^e$ and $\lambda_b \tilde{g}^e$. Numerical results on CP-violating quantities in this scenario are shown in the upper rows of Table II, all smaller than 10^{-4} . The sizes of A_{CP} are significantly smaller than the ones of D meson by an order [3]. One wonders if enhanced CP-violating effect can appear as those showed up in $D \rightarrow \pi^+ \pi^-, K^+ K^-$. If this indeed happens, it must come from \tilde{f}_3 and \tilde{g}_3 .

To estimate how large the effects of \tilde{f}_3 and \tilde{g}_3 are, we adopt a model analysis combining tree level factorization and final state re-scattering (FSR) effects with

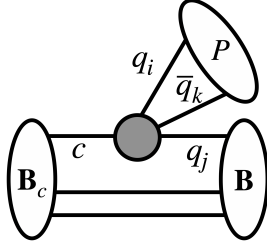


Fig. 1. Topological diagram for $\mathcal{L}_{\mathbf{B}_c\mathbf{B}P}^{\text{Tree}}$, where the middle blob indicates the insertion of $\mathcal{L}_{eff}^{\text{SCS}}$.

$$\begin{aligned} \langle \mathbf{B}P | \mathcal{L}_{\mathbf{B}_c\mathbf{B}P}^{\text{Tree}} | \mathbf{B}_c \rangle &= \frac{G_F}{\sqrt{2}} \left[C_+(\mathcal{H}_+)_k^{ij} + C_-(\mathcal{H}_-)_k^{ij} \right] \langle P | \bar{q}_i \gamma_\mu \gamma_5 q^k | 0 \rangle \langle \mathbf{B} | \bar{q}_j \gamma^\mu (1 - \gamma_5) c | \mathbf{B}_c \rangle \\ &+ \frac{G_F}{\sqrt{2}} \left[C_+(\mathcal{H}_+)_k^{ij} - C_-(\mathcal{H}_-)_k^{ij} \right] \langle P | (\bar{q}_i)_\sigma \gamma_\mu \gamma_5 (q^k)_\rho | 0 \rangle \langle \mathbf{B} | (\bar{q}_j)_\rho \gamma^\mu (1 - \gamma_5) c_\sigma | \mathbf{B}_c \rangle. \end{aligned} \quad (8)$$

The second line with color mismatched comes from the Fierz transformation, where σ and ρ are the quark color indices. In the first line, $\langle P | \bar{q}_i \gamma_\mu \gamma_5 q^k | 0 \rangle$ is proportional to the meson's 4-momentum p^μ , and $\langle \mathbf{B} | \bar{q}_j \gamma^\mu (1 - \gamma_5) c | \mathbf{B}_c \rangle$ corresponds to $\bar{u} \gamma_\mu (\mathbf{a} - \mathbf{b} \gamma_5) u_c$. Their product is proportional to $\bar{u} (M_i - M_f) \mathbf{a} + (M_i + M_f) \mathbf{b} \gamma_5 u_c$. By using the completeness relation of Gell-mann matrices $\sum_a (\lambda_a)_j^i (\lambda_a)_l^k = \delta_l^i \delta_j^k - \delta_j^i \delta_l^k / 3$, the contribution from Fierz transformation is suppressed by 1/3 in the vacuum saturation approximation. To partially taken into account non-factorizable contribution, one replaces 1/3 by $1/N_{eff}$ and let N_{eff} be fixed by data [24, 25]. Observe that the first and second lines in Eq. (8) have the same flavor structures; for the S wave we arrive at

$$\begin{aligned} \mathcal{L}_{\mathbf{B}_c\mathbf{B}P}^{\text{Tree}} &= \sum_{P, \mathbf{B}, \mathbf{B}_c} F_{\mathbf{B}_c\mathbf{B}P}^{\text{Tree}} P^\dagger \bar{\mathbf{B}} \mathbf{B}_c \quad (9) \\ &= (P^\dagger)_i^k (\bar{\mathbf{B}})_j^l \left(\tilde{F}_V^+(\mathcal{H}_+)_k^{ij} + \tilde{F}_V^-(\mathcal{H}_-)_k^{ij} \right) (\mathbf{B}_c)_l. \end{aligned}$$

The parameters \tilde{F}_V^+ and \tilde{F}_V^- present the overall unknowns including \mathbf{a} , the applicable energy scale of C_\pm and N_{eff} . Replacing \tilde{F}_V^\pm by \tilde{G}_A^\pm and inserting γ_5 , we obtain the result for P wave, which will be determined from data.

Note that **15**, $\bar{\mathbf{6}}$ and **3** share two parameters in $\mathcal{L}_{\mathbf{B}_c\mathbf{B}P}^{\text{Tree}}$. Once **15** and $\bar{\mathbf{6}}$ $SU(3)_F$ invariant amplitudes are determined, the amplitudes for **3** are also fixed.

Since the FSR is induced by $\mathcal{L}_{\mathbf{B}_c\mathbf{B}P}^{\text{Tree}}$, Eq. (9) allows us to relate the contributions of **3** to those of $\bar{\mathbf{6}}$ in $\mathcal{L}_{\mathbf{B}_c\mathbf{B}P}^{\text{FSR-s}}$ and $\mathcal{L}_{\mathbf{B}_c\mathbf{B}P}^{\text{FSR-t}}$. We provide some details now. The $s(t)$ -channel FSR diagram is given in Fig. 2a(2b) with the blob representing the SD weak transition induced by $\mathcal{L}_{\mathbf{B}_c\mathbf{B}P}^{\text{Tree}}$. The other vertices are strong couplings among the hadrons

the lowest-lying intermediate baryons of both parities. Within this framework, the full effective Lagrangian for $\mathbf{B}_c \rightarrow \mathbf{B}P$ at hadron level is decomposed into three parts

$$\mathcal{L}_{\mathbf{B}_c\mathbf{B}P} = \mathcal{L}_{\mathbf{B}_c\mathbf{B}P}^{\text{Tree}} + \mathcal{L}_{\mathbf{B}_c\mathbf{B}P}^{\text{FSR-s}} + \mathcal{L}_{\mathbf{B}_c\mathbf{B}P}^{\text{FSR-t}}. \quad (7)$$

The first term is induced by the SD tree-level weak transition depicted in Fig. 1, while the second(third) is responsible for the LD $s(t)$ -channel re-scattering depicted in Fig. 2.

To the leading order, the tree-level $\mathcal{L}_{\mathbf{B}_c\mathbf{B}P}^{\text{Tree}}$ is given by the factorizable contributions

induced by $\mathcal{L}_{\mathbf{B}\mathbf{B}'P}^{\text{strong}}$:

$$\begin{aligned} &\sum_{\mathbf{B}', P} \left(\sum_{\mathbf{B}_+} g_{\mathbf{B}_+\mathbf{B}'P} P^\dagger \bar{\mathbf{B}}' \gamma_5 \mathbf{B}_+ + \sum_{\mathbf{B}_-} g_{\mathbf{B}_-\mathbf{B}'P} P^\dagger \bar{\mathbf{B}}' \mathbf{B}_- \right) + (H.c.) \\ &= g_+ \left((P^\dagger)_j^i (\bar{\mathbf{B}}')_k^j \gamma_5 (\mathbf{B}_+)_i^k + r_+ (P^\dagger)_k^j (\bar{\mathbf{B}}')_j^i \gamma_5 (\mathbf{B}_+)_i^k \right) \quad (10) \\ &+ g_- \left((P^\dagger)_j^i (\bar{\mathbf{B}}')_k^j (\mathbf{B}_-)_i^k + r_- (P^\dagger)_k^j (\bar{\mathbf{B}}')_j^i (\mathbf{B}_-)_i^k \right) + (H.c.), \end{aligned}$$

where the subscript of \pm denotes the parity of \mathbf{B} , and g_\pm and r_\pm are some constants. Generally, the couplings are momenta dependent. We take r_\pm as constants here for estimate.

To determine r_+ , we use the input of $g_{n\Sigma-K^+} = 1.89$ and $g_{p\Lambda K^+} = -3.04$ from the Taylor series extrapolation [26], which yield $r_+ \approx 2.47$. For r_- , we examine the experimental two-body decay widths of $N(1535) \rightarrow N\pi$, $\Sigma(1620) \rightarrow N\bar{K}, \Lambda\pi, \Sigma\pi$, and $\Lambda(1670) \rightarrow N\bar{K}, \Sigma\pi$ with $N \in \{p, n\}$, $\Sigma \in \{\Sigma^\pm, \Sigma^0\}$, $\pi \in \{\pi^\pm, \pi^0\}$ and $\bar{K} \in \{K^-, \bar{K}^0\}$ [27]. Using the decay widths are proportional to the square of the couplings, the best fit solution yields $r_- \approx 2.56$. Here, the values of g_\pm do not concern us as they will be absorbed into the overall unknowns.

Viewing Fig. 2a, we see $\mathcal{L}_{\mathbf{B}_c\mathbf{B}P}^{\text{FSR-s}}$ is made of one $\mathcal{L}_{\mathbf{B}_c\mathbf{B}P}^{\text{Tree}}$ and two $\mathcal{L}_{\mathbf{B}_1\mathbf{B}_2P}^{\text{strong}}$. Contracting the hadron operators according to Fig. 2a, $\langle \mathcal{L}_{\mathbf{B}_c\mathbf{B}P}^{\text{FSR-s}} \rangle$ is proportional to

$$\left\langle (g_{\mathbf{B}_I\mathbf{B}P} P^\dagger \bar{\mathbf{B}} \mathbf{B}_I) (g_{\mathbf{B}_I\mathbf{B}'P'}^* P' \bar{\mathbf{B}}_I \mathbf{B}') (F_{\mathbf{B}_c\mathbf{B}'P'}^{\text{Tree}} P'^t \bar{\mathbf{B}}' \mathbf{B}_c) \right\rangle, \quad (11)$$

where summation over all hadrons is understood. The first, second and third parentheses are the vertices from right to left in Fig. 2a, respectively. The connected lines are the hadron propagators, which are the same for all decays under $SU(3)_F$. We took the S wave as an instance so \mathbf{B}_I must be $J^P = \frac{1}{2}^-$ due to the parity conservation of strong interaction. Likewise, for t -channel $\langle \mathcal{L}_{\mathbf{B}_c\mathbf{B}P}^{\text{FSR-t}} \rangle$ is

proportional to

$$\langle (g_{\mathbf{B}\mathbf{B}'_I P'}^* \overline{P}_1 \overline{\mathbf{B}} \mathbf{B}_I) (g_{\mathbf{B}'_I P'} P^\dagger \overline{\mathbf{B}}_I \mathbf{B}') (F_{\mathbf{B}_c \mathbf{B}'_I P'}^{\text{Tree}} P'^\dagger \overline{\mathbf{B}} \mathbf{B}_c) \rangle. \quad (12)$$

The one of \mathbf{B}_I with positive parity is obtained by insert-

$$\langle \mathcal{L}_{\mathbf{B}_c \mathbf{B} P}^{\text{FSR-s}} \rangle \propto \sum_{\mathbf{B}', P', \mathbf{B}_I} \langle ((P^\dagger)_{j_1}^{i_1} (\overline{\mathbf{B}})_{k_1}^{j_1} (\mathbf{B}_I)_{i_1}^{k_1}) ((P')_{j_2}^{i_2} (\overline{\mathbf{B}}_I)_{k_2}^{j_2} (\mathbf{B}')_{i_2}^{k_2}) ((P'^\dagger)_i^k (\overline{\mathbf{B}}')_j^l (\mathcal{H}_-)^{ij} (\mathbf{B}_c)_l) \rangle, \quad (13)$$

with $i_{1,2}, j_{1,2}, k_{1,2} \in \{1, 2, 3\}$. In our framework, the contributions of \mathcal{H}_+ in $\mathcal{L}_{\mathbf{B}_c \mathbf{B} P}^{\text{FSR-s}(t)}$ vanish due to the KPW theorem. To proceed further, we replace $\sum_{\mathbf{B}'} (\mathbf{B}')_{i_2}^{k_2} (\overline{\mathbf{B}}')_j^l$ by $\sum_a (\lambda_a)_{i_2}^{k_2} (\lambda_a^\dagger)_j^l$ because \mathbf{B}' belongs to $\mathbf{8}$ and is contracted. Likewise, $\sum_{P'} (P')_{j_2}^{i_2} (P'^\dagger)_i^k$ and $\sum_{\mathbf{B}_I} (\overline{\mathbf{B}}_I)_{k_2}^{j_2} (\mathbf{B}_I)_{i_1}^{k_1}$ are replaced by $\sum_a (\lambda_a)_{j_2}^{i_2} (\lambda_a^\dagger)_i^k$ and $\sum_a (\lambda_a^\dagger)_{k_2}^{j_2} (\lambda_a)_{i_1}^{k_1}$, respectively. Applying the completeness relation for λ_a , we get rid of the intermediate hadron operators in Eq. (13) up to an overall factor, which is assigned as \tilde{S}^- . Note that \tilde{S}^- contains unknown information regarding the momenta dependencies of \tilde{F}_V^- and g_\pm in loop integrals. Consequently, we treat it as an independent parameter.

Adding back the r_- term in Eq. (10) and carrying out the same reduction rules for $\mathcal{L}_{\mathbf{B}_c \mathbf{B} P}^{\text{FSR-t}}$, we match Eq. (7) to (6) and find

$$\begin{aligned} \tilde{f}^b &= \tilde{F}_V^- + \tilde{S}^- - \sum_{\lambda=\pm} (2r_\lambda^2 - r_\lambda) \tilde{T}_\lambda^-, \\ \tilde{f}^c &= r_- \tilde{S}^- - \sum_{\lambda=\pm} (r_\lambda^2 - 2r_\lambda + 3) \tilde{T}_\lambda^-, \\ \tilde{f}^d &= \tilde{F}_V^- - \sum_{\lambda=\pm} (2r_\lambda^2 - 2r_\lambda - 4) \tilde{T}_\lambda^-, \quad \tilde{f}^e = \tilde{F}_V^+, \\ \tilde{f}_3^b &= \frac{7 - 2r_-}{8r_- + 2} \tilde{S}^- - \sum_{\lambda=\pm} (r_\lambda^2 - 5r_\lambda/2 + 1) \tilde{T}_\lambda^-, \\ \tilde{f}_3^c &= \frac{(r_- + 1)(2r_- - 7)}{24r_- + 6} \tilde{S}^- + \sum_{\lambda=\pm} \frac{1}{6} (r_\lambda^2 + 11r_\lambda + 1) \tilde{T}_\lambda^-, \\ \tilde{f}_3^d &= \frac{r_-(7 - 2r_-)}{8r_- + 2} \tilde{S}^- - \sum_{\lambda=\pm} \frac{1}{2} (r_\lambda + 1)^2 \tilde{T}_\lambda^- - \frac{1}{4} (\tilde{F}_V^+ + 2\tilde{F}_V^-), \end{aligned} \quad (14)$$

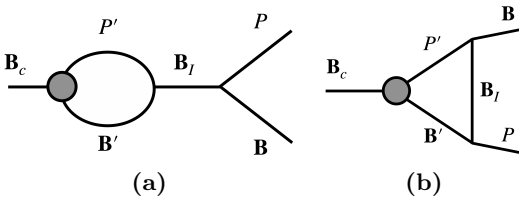


Fig. 2. The left(right) diagram represents the $s(t)$ -channel FSR with the blob representing the SD weak transition induced by $\mathcal{L}_{\mathbf{B}_c \mathbf{B} P}^{\text{Tree}}$.

ing γ_5 into the first two parentheses.

To analyze the flavor structures, we parameterize $g_{\mathbf{B}_I \mathbf{B} P}$ and $F_{\mathbf{B}_c \mathbf{B} P}^{\text{Tree}}$ by Eqs. (9) and (10). For example, we concentrate on $\mathcal{L}_{\mathbf{B}_c \mathbf{B} P}^{\text{FSR-s}}$. The g_+ term in Eq. (10) would not contribute due to the parity. Concentrate on the first term in the last line of Eq. (10), we find

where \tilde{T}_\pm^- represent the overall unknown constants in the t -channel S-wave FSR with the subscript denoting the \mathbf{B}_I parity. The P-wave relations can be obtained by replacing $(\tilde{f}, \tilde{F}_V^\pm, \tilde{S}^-, \tilde{T}_\pm^-, r_\pm)$ by $(-\tilde{g}, \tilde{G}_A^\pm, \tilde{S}^+, \tilde{T}_\pm^+, r_\mp)$ with \tilde{S}^+ (\tilde{T}_\pm^+) an overall unknown in P-wave $s(t)$ -channel FSR. Earlier, we have determined $r_+ \approx 2.47$ and $r_- \approx 2.56$. We take $r_- = r_+$ to combine the summations in Eq. (14) and redefine $\tilde{T}^\pm = (\tilde{T}_+^\pm + \tilde{T}_-^\pm)$.

We are left with the unknown parameters of $(\tilde{F}_V^\pm, \tilde{S}^-, \tilde{T}^-)$ and $(\tilde{G}_A^\pm, \tilde{S}^+, \tilde{T}^+)$. They can be solved by using the input of $\tilde{f}^{b,c,d,e}$ and $\tilde{g}^{b,c,d,e}$ from global fit to $\mathbf{B}_c \rightarrow \mathbf{B} P$ [20]. After that, we obtain \tilde{f}_3 and \tilde{g}_3 in Table I. We see that their absolute values are in the same size with $\tilde{f}^{b,c,d,e}$ and $\tilde{g}^{b,c,d,e}$, which may lead to a large CP violation.

The predicted A_{CP} and A_{CP}^α are collected in the lower rows of Table II. The A_{CP} are typically enhanced to the size of 10^{-3} in accordance with the enhanced CP violation in D meson decay. The CP asymmetries of $\Lambda_c^+ \rightarrow p\pi^0, n\pi^+$ are large, but the neutral particles in the final states make them challenging to be detected. Remarkably for $\Xi_c^+ \rightarrow \Xi^0 K^+$, $\mathcal{B} = (1.04 \pm 0.14) \cdot 10^{-3}$ and $A_{CP} = (-1.39 \pm 0.46) \cdot 10^{-3}$ are both sizable which may be more promising.

Under the U-spin symmetry, an $SU(2)$ subgroup of $SU(3)_F$ between d and s , exchanging d and s in the initial and final states, can be effectively viewed as taking the transformation of $(\lambda_s - \lambda_d, \lambda_b) \rightarrow (-\lambda_s + \lambda_d, \lambda_b)$. Since CP asymmetries are proportional to $\text{Im}(\lambda_b^* (\lambda_s - \lambda_d))$, they flip signs after exchanging d and s in the initial and final states. This kind of $SU(3)_F$ relations provide useful information to test the CKM mechanism model-independently [28]. Explicitly, from U-spin symmetry we have [14, 29]

$$\begin{aligned} A_{CP}(\Lambda_c^+ \rightarrow \Sigma^+ K_{S/L}^0) &= -A_{CP}(\Xi_c^+ \rightarrow p K_{S/L}^0), \\ A_{CP}(\Lambda_c^+ \rightarrow n\pi^+) &= -A_{CP}(\Xi_c^+ \rightarrow \Xi^0 K^+), \\ A_{CP}(\Xi_c^0 \rightarrow \Xi^0 K_{S/L}^0) &= -A_{CP}(\Xi_c^0 \rightarrow n K_{S/L}^0), \\ A_{CP}(\Xi_c^0 \rightarrow \Sigma^- \pi^+) &= -A_{CP}(\Xi_c^0 \rightarrow \Xi^- K^+), \\ A_{CP}(\Xi_c^0 \rightarrow \Sigma^+ \pi^-) &= -A_{CP}(\Xi_c^0 \rightarrow p K^-). \end{aligned} \quad (15)$$

The relations also apply when substituting A_{CP}^α for A_{CP} .

Table I The values of the $SU(3)_F$ parameters where $\tilde{h} = |\tilde{h}| \exp(i\delta_h)$ with $\tilde{h} \in \{\tilde{f}_{\mathbf{3}}^{b,c,d,e}, \tilde{g}_{\mathbf{3}}^{b,c,d,e}\}$. The values of $\tilde{f}_{\mathbf{3}}^{b,c,d,e}$ and $\tilde{g}_{\mathbf{3}}^{b,c,d,e}$ are collected from Ref. [20], while the ones of $\tilde{f}_{\mathbf{3}}$ and $\tilde{g}_{\mathbf{3}}$ from solving Eq. (14). The $|\tilde{h}|$ and δ_h are in units of $10^{-2}G_F\text{GeV}^2$ and radians, respectively. Values within parentheses represent the backward digit count of uncertainties, such as $3.64(1.20) = 3.64 \pm 1.20$.

	\tilde{f}^b	\tilde{f}^c	\tilde{f}^d	\tilde{f}^e	$\tilde{f}_{\mathbf{3}}^b$	$\tilde{f}_{\mathbf{3}}^c$	$\tilde{f}_{\mathbf{3}}^d$
$ \tilde{h} $	3.64(1.20)	3.84(0.18)	1.25(1.24)	2.19(2.52)	0.54(13)	4.40(96)	5.46(1.33)
δ_h	0	-2.20(39)	-0.57(31)	-0.58(50)	0.85(23)	-2.19(24)	1.00(38)
	\tilde{g}^b	\tilde{g}^c	\tilde{g}^d	\tilde{g}^e	$\tilde{g}_{\mathbf{3}}^b$	$\tilde{g}_{\mathbf{3}}^c$	$\tilde{g}_{\mathbf{3}}^d$
$ \tilde{h} $	28.05 (1.18)	2.76(1.72)	5.23 (1.55)	6.49(5.35)	3.67(23)	25.90(1.92)	32.34(2.83)
δ_h	2.60(0.37)	2.03(0.43)	2.39(0.74)	1.98(1.03)	3.14(32)	0.01(32)	-3.12(32)

The above U-spin relations help reduce systematic errors and make the observables larger in experiments, in the same spirit as $A_{CP}(D^0 \rightarrow \pi^+\pi^-) - A_{CP}(D^0 \rightarrow K^+K^-)$. Specifically, we recommend to measure $A_{CP}(\Xi_c^0 \rightarrow pK^-) - A_{CP}(\Xi_c^0 \rightarrow \Sigma^+\pi^-)$ and $A_{CP}^\alpha(\Xi_c^0 \rightarrow pK^-) - A_{CP}^\alpha(\Xi_c^0 \rightarrow \Sigma^+\pi^-)$, which, according to our analysis, is found to be $(1.87 \pm 0.57) \cdot 10^{-3}$ and $(-4.94 \pm 0.57) \times 10^{-3}$, respectively. All the final states are charged, making it an ideal channel to probe CP violation.

Data from LHCb revealed significant U-spin breaking in D^0 decays [4], yet good $SU(3)_F$ fits in charmed baryon decays indicate otherwise [20]. Resonances $f(1710)$ and $f(1790)$, close in mass to D^0 , are thought to contribute significantly to $SU(3)_F$ breaking in D^0 decays [30, 31]. Conversely, no similar mechanism is expected in charmed baryon decays. Large deviations from Eq. (15) are not expected, providing valuable tests for the SM.

Before ending the discussions, we would like to comment on the $Q_{3\sim 6}$ effects which have been neglected so far. They will scale the last term $-(\tilde{F}_V^+ + 2\tilde{F}_V^-)/4$ in $\tilde{f}_{\mathbf{3}}^d$ by a factor of $(1 + \mathcal{R}_+)$ with

$$\mathcal{R}_\pm = \frac{(3C_4 + C_3)m_c \pm \frac{2m_K^2}{m_s + m_u}(3C_6 + C_5)}{(C_+ + C_-)m_c}, \quad (16)$$

and similarly $-(\tilde{G}_A^+ + 2\tilde{G}_A^-)/4$ in $\tilde{g}_{\mathbf{3}}^d$ by a factor of $(1 + \mathcal{R}_-)$. We have checked that the corrections on A_{CP} and A_{CP}^α are less than 10%, which can be neglected.

A lot of charmed baryons will be produced in the near future. At the High-Luminosity Super τ -Charm Factory [32], approximately $10^8 \Lambda_c^+$ baryons are expected to be observed [33]. Assuming systematic uncertainties are canceled when subtracting the number of events between Λ_c^+ and Λ_c^- , the experimental precision of A_{CP} may reach a few $\mathcal{O}(10^{-3})$. By far, Belle's data of 1 ab^{-1} provided a precision of A_{CP} and A_{CP}^α at 10^{-2} [34]. Belle II's expected production number is fifty times larger, and its precision can reach 10^{-3} . At LHCb, the production rates of charmed baryons are suppressed to around 30% compared with D mesons [35]. The precision of A_{CP} may also reach 10^{-3} . After the High Luminosity upgrade [36], the integrated luminosity is expected to increase tenfold. The enhancement found in this work allows for the observation of CP violation with high confidence in two-body charmed baryon decays for the first time.

ACKNOWLEDGMENTS

This work is supported in part by the National Key Research and Development Program of China under Grant No. 2020YFC2201501, by the Fundamental Research Funds for the Central Universities, by National Natural Science Foundation of P.R. China (No.12090064, 12205063 and 12375088).

-
- [1] A. D. Sakharov, Pisma Zh. Eksp. Teor. Fiz. **5**, 32-35 (1967).
[2] M. Kobayashi and T. Maskawa, Prog. Theor. Phys. **49**, 652-657 (1973).
[3] R. Aaij *et al.* [LHCb], Phys. Rev. Lett. **122**, no.21, 211803 (2019) [arXiv:1903.08726 [hep-ex]].
[4] R. Aaij *et al.* [LHCb], Phys. Rev. Lett. **131**, no.9, 091802 (2023) [arXiv:2209.03179 [hep-ex]].

-
- [5] A. Lenz and G. Wilkinson, Ann. Rev. Nucl. Part. Sci. **71**, 59-85 (2021) [arXiv:2011.04443 [hep-ph]].
[6] R. Bause, H. Gisbert, G. Hiller, T. Höhne, D. F. Litim and T. Steudtner, Phys. Rev. D **108**, no.3, 035005 (2023) [arXiv:2210.16330 [hep-ph]].
[7] S. Schacht, JHEP **03**, 205 (2023) [arXiv:2207.08539 [hep-ph]].
[8] H. Y. Cheng and C. W. Chiang, Phys. Rev. D **100**, no.9,

Table II The predicted values of \mathcal{B} , A_{CP} and A_{CP}^α in units of 10^{-3} . The upper rows of A_{CP} and A_{CP}^α are obtained by taking $\tilde{f}_3^{b,c,d} = \tilde{g}_3^{b,c,d} = 0$, while the lower rows by the FSR mechanism.

Channels	\mathcal{B}	A_{CP}^α	A_{CP}	Channels	\mathcal{B}	A_{CP}^α	A_{CP}
$\Lambda_c^+ \rightarrow p\pi^0$	0.16(2)	-0.61(39) -3.39(1.05)	0.42(1.15) 1.08(1.55)	$\Xi_c^0 \rightarrow \Sigma^+\pi^-$	0.21(2)	0 2.27(22)	0 -0.86(25)
$\Lambda_c^+ \rightarrow n\pi^+$	0.67(8)	0.12(20) -1.27(1.07)	-0.15(42) 1.41(68)	$\Xi_c^0 \rightarrow \Sigma^0\pi^0$	0.34(3)	-0.04(12) 0.35(9)	-0.12(43) -0.11(11)
$\Lambda_c^+ \rightarrow \Lambda^0 K^+$	0.63(2)	-0.03(10) -0.46(14)	0.19(18) -0.13(25)	$\Xi_c^0 \rightarrow \Sigma^-\pi^+$	1.83(6)	0.02(7) -0.03(4)	0.13(21) 0.05(7)
$\Xi_c^+ \rightarrow \Sigma^+\pi^0$	2.12(14)	0.06(13) 0.21(10)	-0.32(36) 0.02(18)	$\Xi_c^0 \rightarrow \Xi^0 K_{S/L}$	0.43(2)	0 0.28(2)	0 -0.12(3)
$\Xi_c^+ \rightarrow \Sigma^0\pi^+$	3.04(10)	-0.01(6) 0.15(7)	0.17(19) 0.08(13)	$\Xi_c^0 \rightarrow \Xi^- K^+$	1.12(3)	0.02(5) 0.03(4)	0.10(14) -0.06(6)
$\Xi_c^+ \rightarrow \Xi^0 K^+$	1.04(14)	0.02(14) 1.22(78)	-0.19(28) -1.39(46)	$\Xi_c^0 \rightarrow pK^-$	0.20(2)	0 -2.67(35)	0 1.01(32)
$\Xi_c^+ \rightarrow \Lambda^0\pi^+$	0.32(9)	0.0(19) 1.40(34)	-0.15(49) -0.02(43)	$\Xi_c^0 \rightarrow nK_{S/L}$	0.71(6)	0 -0.27(2)	0 0.11(3)
$\Xi_c^0 \rightarrow \Lambda^0\pi^0$	0.09(1)	0.07(20) 0.89(22)	0.12(38) -0.39(23)				

- 093002 (2019) [arXiv:1909.03063 [hep-ph]].
- [9] I. Bediaga, T. Frederico and P. C. Magalhães, Phys. Rev. Lett. **131**, no.5, 051802 (2023) [arXiv:2203.04056 [hep-ph]].
- [10] A. Pich, E. Solomonidi and L. Vale Silva, Phys. Rev. D **108**, no.3, 036026 (2023) [arXiv:2305.11951 [hep-ph]].
- [11] T. D. Lee and C. N. Yang, Phys. Rev. **108**, 1645-1647 (1957).
- [12] G. Buchalla, A. J. Buras and M. E. Lautenbacher, Rev. Mod. Phys. **68**, 1125-1144 (1996) [arXiv:hep-ph/9512380 [hep-ph]].
- [13] M. Ablikim *et al.* [BESIII], Phys. Rev. Lett. **132**, no.3, 031801 (2024) [arXiv:2309.02774 [hep-ex]].
- [14] X. G. He, Y. J. Shi and W. Wang, Eur. Phys. J. C **80**, no.5, 359 (2020) [arXiv:1811.03480 [hep-ph]].
- [15] T. M. Yan, H. Y. Cheng, C. Y. Cheung, G. L. Lin, Y. C. Lin and H. L. Yu, Phys. Rev. D **46**, 1148-1164 (1992) [erratum: Phys. Rev. D **55**, 5851 (1997)].
- [16] C. Q. Geng, C. W. Liu and T. H. Tsai, Phys. Lett. B **794**, 19-28 (2019) [arXiv:1902.06189 [hep-ph]].
- [17] F. Huang, Z. P. Xing and X. G. He, JHEP **03**, 143 (2022) [erratum: JHEP **09**, 087 (2022)] [arXiv:2112.10556 [hep-ph]].
- [18] H. Zhong, F. Xu, Q. Wen and Y. Gu, JHEP **02**, 235 (2023) [arXiv:2210.12728 [hep-ph]].
- [19] Z. P. Xing, X. G. He, F. Huang and C. Yang, Phys. Rev. D **108**, no.5, 053004 (2023).
- [20] C. Q. Geng, X. G. He, X. N. Jin, C. W. Liu and C. Yang, Phys. Rev. D **109**, no.7, L071302 (2024) [arXiv:2310.05491 [hep-ph]].
- [21] H. Zhong, F. Xu and H. Y. Cheng, [arXiv:2401.15926 [hep-ph]]; H. Zhong, F. Xu and H. Y. Cheng, [arXiv:2404.01350 [hep-ph]].
- [22] H. n. Li, C. D. Lu and F. S. Yu, Phys. Rev. D **86**, 036012 (2012) [arXiv:1203.3120 [hep-ph]].
- [23] J. G. Körner, Nucl. Phys. B **25**, 282-290 (1971); J. C. Pati and C. H. Woo, Phys. Rev. D **3**, 2920-2922 (1971); S. Groote and J. G. Körner, Eur. Phys. J. C **82**, no.4, 297 (2022) [arXiv:2112.14599 [hep-ph]].
- [24] A. J. Buras, J. M. Gerard and R. Ruckl, Nucl. Phys. B **268**, 16-48 (1986).
- [25] M. Bauer, B. Stech and M. Wirbel, Z. Phys. C **34**, 103 (1987).
- [26] I. J. General and S. R. Cotanch, Phys. Rev. C **69**, 035202 (2004) [arXiv:nucl-th/0311039 [nucl-th]].
- [27] R. L. Workman *et al.* [Particle Data Group], PTEP **2022**, 083C01 (2022).
- [28] N. G. Deshpande and X. G. He, Phys. Rev. Lett. **75**, 1703-1706 (1995) [arXiv:hep-ph/9412393 [hep-ph]].
- [29] D. Wang, Eur. Phys. J. C **79**, no.5, 429 (2019) [arXiv:1901.01776 [hep-ph]].
- [30] H. Y. Cheng and C. W. Chiang, Phys. Rev. D **81**, 074021 (2010) [arXiv:1001.0987 [hep-ph]].
- [31] S. Schacht and A. Soni, Phys. Lett. B **825**, 136855 (2022) [arXiv:2110.07619 [hep-ph]].
- [32] M. Achasov, X. C. Ai, R. Aliberti, L. P. An, Q. An, X. Z. Bai, Y. Bai, O. Bakina, A. Barnyakov and V. Blinov, *et al.* Front. Phys. (Beijing) **19**, no.1, 14701 (2024) [arXiv:2303.15790 [hep-ex]].
- [33] H. Y. Cheng, X. R. Lyu and Z. Z. Xing, [arXiv:2203.03211 [hep-ph]].
- [34] L. K. Li *et al.* [Belle], Sci. Bull. **68**, 583-592 (2023) [arXiv:2208.08695 [hep-ex]].
- [35] R. Aaij *et al.* [LHCb], JHEP **02**, 102 (2019) [arXiv:1809.01404 [hep-ex]].
- [36] G. Apollinari, I. Béjar Alonso, O. Brüning, P. Fessia, M. Lamont, L. Rossi and L. Taviani, ‘High-Luminosity Large Hadron Collider (HL-LHC): Technical Design Report V. 0.1,’ doi:10.23731/CYRM-2017-004.